UNIVERSITY OF LEEDS

This is a repository copy of *Gamma and beta frequency oscillations in response to novel auditory stimuli: A comparison of human electroencephalogram (EEG) data with in vitro models* .

White Rose Research Online URL for this paper:
http://eprints.whiterose.ac.uk/567/

Article:
Haenschel, C., Baldeweg, T., Croft, R.J. et al. (2 more authors) (2000) Gamma and beta frequency oscillations in response to novel auditory stimuli: A comparison of human electroencephalogram (EEG) data with in vitro models. Proceedings of the National Academy of Sciences, 97 (13). pp. 7645-7650. ISSN 0027-8424

https://doi.org/10.1073/pnas.120162397

Reuse
Unless indicated otherwise, fulltext items are protected by copyright with all rights reserved. The copyright exception in section 29 of the Copyright, Designs and Patents Act 1988 allows the making of a single copy solely for the purpose of non-commercial research or private study within the limits of fair dealing. The publisher or other rights-holder may allow further reproduction and re-use of this version - refer to the White Rose Research Online record for this item. Where records identify the publisher as the copyright holder, users can verify any specific terms of use on the publisher's website.

Takedown
If you consider content in White Rose Research Online to be in breach of UK law, please notify us by emailing eprints@whiterose.ac.uk including the URL of the record and the reason for the withdrawal request.

White Rose university consortium
Universities of Leeds, Sheffield & York

eprints@whiterose.ac.uk
https://eprints.whiterose.ac.uk/

Gamma and beta frequency oscillations in response to novel auditory stimuli: A comparison of human electroencephalogram (EEG) data with *in vitro* models

Corinna Haenschel*†, Torsten Baldeweg‡, Rodney J. Croft*, Miles Whittington§, and John Gruzelier*

*Division of Neuroscience and Psychological Medicine, Imperial College School of Medicine, London W6 8RP, United Kingdom; ‡Institute of Child Health and Great Ormond Street Hospital for Sick Children, University College London, London WC1N 2AP, United Kingdom; and §School of Biomedical Sciences, University of Leeds, Leeds LS2 9NL, United Kingdom

Communicated by Nancy J. Kopell, Boston University, Boston, MA, April 10, 2000 (received for review December 15, 1999)

Investigations using hippocampal slices maintained *in vitro* have demonstrated that bursts of oscillatory field potentials in the gamma frequency range (30–80 Hz) are followed by a slower oscillation in the beta 1 range (12–20 Hz). In this study, we demonstrate that a comparable gamma-to-beta transition is seen in the human electroencephalogram (EEG) in response to novel auditory stimuli. Correlations between gamma and beta 1 activity revealed a high degree of interdependence of synchronized oscillations in these bands in the human EEG. Evoked (stimulus-locked) gamma oscillations preceded beta 1 oscillations in response to novel stimuli, suggesting that this may be analogous to the gamma-to-beta shift observed *in vitro*. Beta 1 oscillations were the earliest discriminatory responses to show enhancement to novel stimuli, preceding changes in the broad-band event-related potential (mismatch negativity). Later peaks of induced beta activity over the parietal cortex were always accompanied by an underlying gamma frequency oscillation as seen *in vitro.* A further analogy between *in vitro* and human recordings was that both gamma and beta oscillations habituated markedly after the initial novel stimulus presentation.

Gamma and beta frequency oscillations occur in the neocortex in response to sensory stimuli over a range of modalities (1, 2). Evidence is accumulating that gamma oscillations are involved in feature binding and associational memory (3, 4). The mechanism behind these cortical oscillations remains to be elucidated, but research has demonstrated that, at a cellular and network level, cortical gamma activity can be generated by specific neuronal subtypes (5) and networks of interconnected inhibitory interneurons (6). At a larger network level, focal cortical gamma oscillations can be elicited upstream from primary sensory pathways by tetanic stimulation of the thalamic reticular nucleus (7). Previous studies using cortical and hippocampal slice preparations have demonstrated that experimental gamma oscillations can occur spontaneously for long periods of time during activation of metabotropic cholinergic receptors (8) and can be induced transiently by activation of metabotropic glutamate receptors or by bursts of afferent stimulation (6, 9, 10).

Experimentally, beta frequency oscillations are generated following periods of synchronous gamma frequency activity (9, 10). Their generation depends on the period-by-period potentiation of recurrent excitatory synaptic potentials, which occurs concurrently with a recovery of postspike afterhyperpolarization following the initial stimulus. The beta oscillations appeared to manifest as subharmonics of the preceding gamma oscillation, with pyramidal cells firing on only every second or third period of a continuing subthreshold, inhibition-based gamma oscillation. As a consequence, all cells involved in the beta network will skip the same beats. These oscillations have been suggested to represent a dynamic method of generating and recalling stimulus-specific assemblies of neurons. In addition, recent efforts to model beta oscillations have shown that their generation enhances the range of temporal delays between elements in a neuronal assembly within which synchronization is possible (11). This observation is complementary to the demonstration that long-range (multimodal) sensory coding is performed at beta frequencies, whereas local synchronization occurs at gamma frequencies (12).

Transient bursts of gamma oscillations in the human electroencephalogram (EEG) can be detected in response to sensory stimulation (13). They can either be tightly time and phase locked to the stimulus (termed stimulus-evoked gamma oscillations) (14), or they may occur with variable latency (termed stimulus-induced gamma oscillations) (15). Stimulus-evoked gamma oscillations are contained in the averaged evoked potential and can be extracted by band-pass filtering (14). Such short-latency gamma-band oscillations have been found in the auditory potential within 100 ms from stimulus onset (16–19). In contrast, stimulus-induced gamma oscillations disappear in the average evoked potential because of the jitter in latency from one trial to the next. They have to be extracted by using methods that distinguish between phase-locked and non-phase-locked activity (20). In this study, we used the method of event-related synchronization and desynchronization (21).

Induced gamma activity has been found in response to sensory stimuli in the human EEG (15, 20). The functional significance of evoked and induced gamma oscillations still remains unclear. However, it has been suggested that the evoked gamma band response may reflect synchronously active neural assemblies (feature binding) or may signal the precise temporal relationship of concurrently incoming stimuli (20). The later induced gamma oscillation is thought to reflect object representation (3, 20) or the activation of associative memories (4, 22).

Recent *in vitro* studies have demonstrated that stimulus-induced gamma and beta oscillations habituate markedly on repeated stimulation (23). The aim of this study was to investigate the relationship between gamma and beta oscillations in the human EEG in response to novel and repeated auditory stimuli designed to mimic the *in vitro* paradigm. We tested the hypothesis that novel stimuli differing in frequency from a repeated sequence of tones would elicit a similar burst of correlated gamma and beta 1 activity. Furthermore, we expected that these responses, particularly with regard to induced oscillations, would habituate rapidly with stimulus repetition.

Methods

Subjects. Ten participants (three females, seven males), 20–35 years old (mean, 21.5), with normal hearing were tested. All

Abbreviations: EEG, electroencephalogram; ERP, event-related potential; GFP, global field power; MMN, mismatch negativity.

†To whom reprint requests should be addressed at: Cognitive Neuroscience and Behavior, Imperial College School of Medicine, London W6 8RP, UK. E-mail: C.Haenschel@ic.ac.uk.

The publication costs of this article were defrayed in part by page charge payment. This article must therefore be hereby marked "*advertisement*" in accordance with 18 U.S.C. §1734 solely to indicate this fact.

Article published online before print: *Proc. Natl. Acad. Sci. USA*, 10.1073/pnas.120162397. Article and publication date are at www.pnas.org/cgi/doi/10.1073/pnas.120162397

participants were free of neurological and psychiatric disorders and had no history of hearing impairment. Ethical approval was obtained and all participants provided written consent before testing. Subjects were seated in an armchair with head support in a sound-attenuated and electrically shielded testing chamber. Instructions were given to relax completely with eyes closed.

Stimuli. Pure sinusoidal tones were generated with a Neurosoft Sound program and delivered binaurally through headphones by the Stim interface system (Neuroscan Labs, Sterling, VA). Stimuli were presented in a series of 40 trials. A single trial consisted of a sequence of 8 tones (randomized up to a maximum of 16) of one constant frequency, of which the first eight were analyzed. The tone frequency altered randomly between trials from the lower frequency limit of 100 Hz to the upper limit of 5000 Hz (from 100 to 1000 Hz in steps of 100 Hz and between 1000 and 5000 Hz in steps of 200 Hz). The tones were 50 ms long (rise and fall time 5 ms), had an intensity of 95 dB (sound pressure level), and were presented with a constant stimulus onset asynchrony of 2 s. The intertrial interval was also 2 s.

EEG Recording. An ECI Electro-Cap containing 28 electrodes arranged in accordance with the international 10–20 system was fitted to the subject's head and a ground electrode was placed 1.5 cm in front of the central frontal electrode. A reference electrode was attached to the nose. Vertical and horizontal electrooculogram electrodes were placed above and below the right eye and laterally from both eyes. Recording, digitization, and processing of the EEG data were carried out with a SynAmps amplifier and Neuroscan system version 4.0. The EEG was recorded at a sampling rate of 500 Hz with a system bandpass between 0 and 100 Hz.

Data Analysis. EEG data were averaged in intervals from 500 ms before the stimulus and up to 1,000 ms after stimulus onset and were baseline corrected from −250 to 0 ms before stimulus for each stimulus. First, EEG epochs were excluded automatically if amplitudes exceeded ±100 μV and were then visually inspected for more subtle artifacts, such as muscle contamination.

Broad-band event-related potential (ERP) components were filtered between 0.5 and 30 Hz before further processing. Peak amplitudes and latencies of N1 and P3 components were defined in the following time intervals: 80–150 ms and 250–450 ms, respectively. Analysis of oscillatory responses distinguished between phase-locked and non-phase-locked activity. In both sets of analyses, the cut-off frequencies for the following frequency bands were as follows: alpha, 8–12 Hz; beta 1, 12–20 Hz; beta 2, 20–30 Hz; and gamma, 30–50 Hz. No specific predictions were made for changes in the alpha band. However, it was included in the analysis to exclude the possibility that changes in the gamma band may be artifacts of alpha harmonics (16).

Stimulus-evoked activity was obtained from the averaged evoked potential of each subject by bandpass filtering with a two-pole Butterworth, zero-phase-shift digital filter (−6 dB edges at cut-off frequencies, slope 24 dB/octave). For analysis of evoked oscillatory activity, we used a global field power (GFP) analysis as previously suggested to improve the signal-to-noise ratio of multichannel data (17). GFP is defined as the standard deviation across multiple channels as a function of time. It is a root mean square measure that quantifies the spatial potential field sampled over the scalp. A peak of GFP reflects a maximum of the total underlying brain activity that contributes to the surface potential field (24). GFP was used to measure the mean and peak amplitude as well as latency for stimulus-evoked gamma, beta 1, beta 2, and alpha bands in the 20- to 150-ms time window.

The power of induced activity was calculated by using the Instantaneous Frequency Analysis module of Scan 4.0 software (Neuroscan Labs) based on the method of complex demodulation (25, 26). First, the center frequency (CF) and cut-off frequency were selected for a zero-phase bandpass filter. Complex demodulation then produced a complex time series [with real part $\cos(2\pi \cdot CF \cdot t)$ and imaginary part $\sin(2\pi \cdot CF \cdot t)$] from the original real-time series. This had the effect of shifting the entire spectrum of the original time series to 0 Hz. Both the real and imaginary parts were low-pass filtered. Then the envelope of the center frequency activity was computed as the modulus of the complex time series after filtering (in units of power in μV^2). To compute the induced band power statistic across all epochs, the modulus squared was summed across all epochs, and the real and imaginary parts were summed across all epochs (at each time point within the epoch). The mean across epochs at each time point (average evoked potential) was explicitly removed for the power computations. The result is the event-related induced band power. Mean and peak amplitude as well as latency of the induced oscillations were identified in the time window between 200 and 400 ms and 600 and 800 ms in response to each of the eight tones.

Statistical Analysis. The statistical analyses were based on the *a priori* hypotheses that response habituation in gamma and beta oscillations occurs immediately following the first stimulus as observed in the *in vitro* experiments (23). Therefore, repeated-measures ANOVA compared the response to stimulus 1 with the mean of subsequent stimuli 2–8 (within-subject factor stimulus). To account for possible topographical effects on broad-band ERP components N1 and P3 as well as on induced activity in each frequency band, the following within-subject factors were also included: anterior–posterior ($n = 2$) and side ($n = 3$: left, center, right). These six regions included the following electrodes: left anterior region F3, F7, T3, C3; central anterior region CZ, FZ; right anterior region F4, F8, T4, C4; left posterior region P3, T5, PO1; central posterior region PZ, OZ; and right posterior region P4, T6, PO2.

Topographical information was not available for the GFP values (evoked activity). Therefore, *t* tests were used to compare mean GFP differences within each frequency band. Peak latencies were compared to test the hypotheses that evoked and induced gamma oscillations would precede beta activity. Bonferroni correction was applied to correct for multiple comparisons across frequency bands.

Results

Broad-Band ERPs. The first stimulus in each trial evoked enhanced N1 and P3 components ($F_{(1,9)} = 11.4$, $P < 0.001$), $F_{(1,9)} = 32.7$, $P < 0.001$, respectively) (Fig. 1). The corresponding difference waves revealed an early frontal negative wave peaking at 107 ms, which exhibited the typical characteristics of a mismatch negativity (MMN or N2a) (27). In contrast to the later N2b component, which was maximal at the vertex, MMN showed inverted peaks at mastoid electrodes (data not shown). With large frequency separation between stimuli, the MMN temporally overlaps the N1 (28, 29). The P3 component in the difference wave showed a vertex (CZ) amplitude maximum at 322 ms and a later parietal peak at 350 ms.

Evoked Oscillatory Activity. The gamma response to stimulus 1 consisted of a negative-positive-negative complex peaking at 45 ms (SD 16) with a fronto-central distribution (Figs. 2 and 3). This complex showed inverted peaks at temporal leads, in line with previous evidence suggesting bilateral sources within the superior temporal plane (13). The evoked beta 1 and beta 2 responses showed a similar distribution, but with longer peak latencies (74 ms, SD 27 and 59 ms, SD 26, respectively). GFP measurements indicated a steady rise in beta 1 power during the initial burst of gamma activity. As this initial stimulus-locked gamma burst

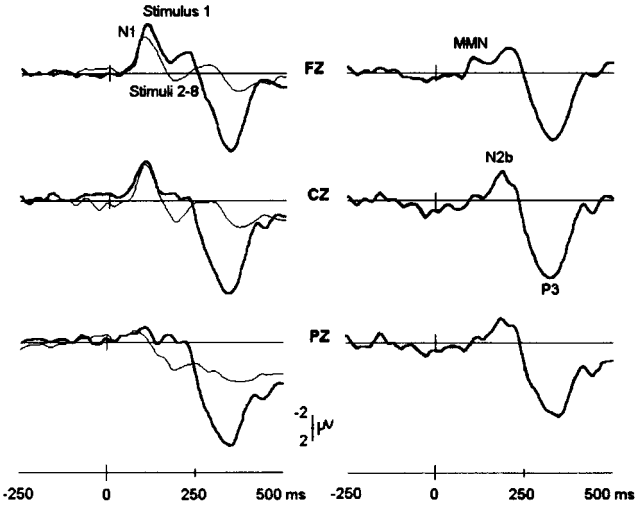

Fig. 1. Broad-band ERPs shown in response to the first stimulus and stimuli 2–8 (*Left*) and corresponding difference waves (*Right*) for fronto-central (FZ, *Top*), vertex (CZ, *Middle*), and centro-parietal (PZ, *Bottom*) electrodes. MMN, mismatch negativity. Note the prominent P3 potential at 320 ms with a vertex maximum compared with the more posterior peak at 350 ms. The former resembles the ''novelty P3'' (P3a) described by Knight and Nakada (30).

subsided, it was replaced by a strong oscillatory response within the beta 1 band. There was a delay of approximately two periods of gamma oscillation before the onset of beta 1 activity. The mean evoked response to stimulus 1 was significantly larger compared with subsequent stimuli (Figs. 2 and 4) for beta 1 ($t_{(9)} = 2.36, P = 0.042$), but not for beta 2 ($t_{(9)} = 1.73, P = 0.118$) and gamma ($t_{(9)} = 1.29, P = 0.230$).

As predicted, activity in the gamma band peaked significantly earlier than in beta 1 ($t_{(9)} = 3.60, P = 0.006$), but not in beta 2 ($t_{(9)} = 1.88, P = 0.093$). The same was true for peak latencies to the subsequent stimuli 2–8 (gamma: 49 ms, SD 12; beta 1: 65 ms, SD 11; beta 2: 50 ms, SD 13; $t_{(9)} = 2.61, P = 0.028$; $t_{(9)} = 0.17$, $P = 0.867$, respectively).

It is important to note that there were no significant stimulus effects for evoked alpha activity ($t_{(9)} = 0.60, P = 0.563$). Also, alpha peaked later (102 ms, SD 40) in comparison to the other frequency bands, and this difference was significant (stimulus 1: $t_{(9)} > 2.84, P < 0.019$; stimuli 2–8: $t_{(9)} > 3.99, P < 0.003$).

Induced Oscillatory Activity. Two distinct peaks of induced activity with a central posterior distribution were seen in response to stimulus 1. As predicted, the first peak of oscillatory-induced activity (200–400 ms; Fig. 2) was larger in response to stimulus 1 compared with subsequent stimuli for beta 1 (stimulus effect, $F_{(1,9)} = 6.2, P = 0.035$); beta 2, ($F_{(1,9)} = 7.1, P = 0.029$) and in trend for gamma: $F_{(1,9)} = 4.9, P = 0.054$). Gamma and beta 1 activity were larger over posterior compared with anterior regions for the first but not for subsequent stimuli (interaction effect stimulus by anterior-posterior) for gamma: $F_{(1,9)} = 6.1$, $P = 0.036$; and beta 1: $F_{(1,9)} = 5.4, P = 0.045$). The habituation of the oscillatory response within these frequency bands occurred after the initial novel stimulus and was not graded throughout consecutive stimuli (Figs. 2 and 4). Similar changes occurred in the second peak of induced gamma and beta 1 activity between 600 and 800 ms poststimulus (stimulus effect: for gamma: $F_{(1,9)} = 7.7, P = 0.022$, beta 1: $F_{(1,9)} = 5.5, P = 0.044$), beta 2 ($F_{(1,9)} = 4.5, P = 0.064$). However, in contrast to the first peak, this later peak was still evident in response to subsequent stimuli. For beta 1 this peak was also more prominent at posterior sites ($F_{(1,9)} = 7.4, P = 0.023$).

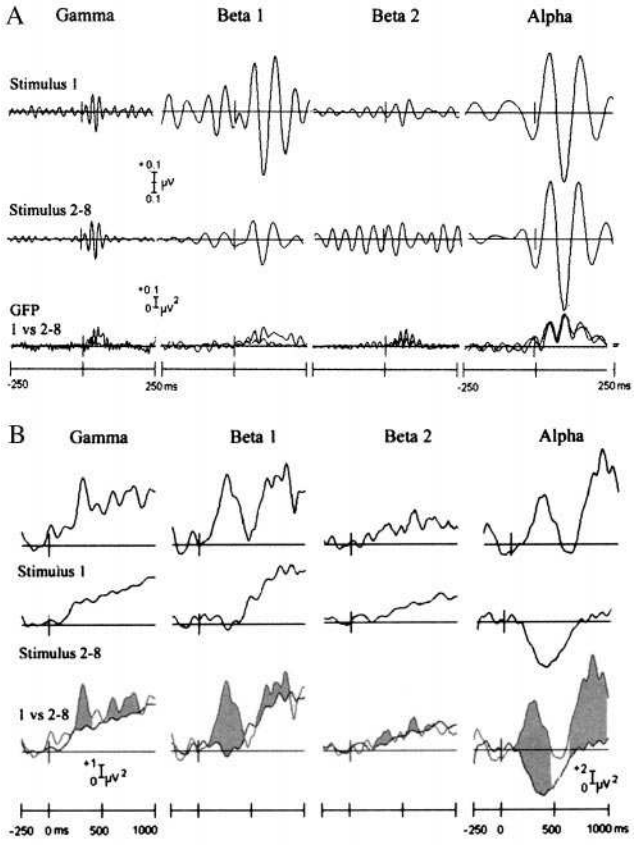

Fig. 2. (*A*) Stimulus-locked oscillations. Grand average auditory evoked responses to stimulus 1 and stimuli 2–8 are shown for gamma (30–50 Hz), beta 1 (12–20 Hz), beta 2 (20–30 Hz), and alpha bands (8–12 Hz). Global Field Power (GFP) quantifies the spatial potential field over the scalp. Note that the GFP values exhibit twice the frequency of the bandpass frequency because of rectification of the data when computing root-mean-square values. (*B*) Induced activity. Time windows used for statistical analysis of the two induced peaks are indicated in shading in the bottom traces.

In contrast to the pattern of peak latencies of the *evoked* oscillatory activity where gamma led beta 1, peaks of *induced* beta activity appeared to superimpose on a prolonged period of induced gamma frequency activity (Fig. 5). The peak latencies of these two induced peaks at the point of maximum (Fig. 2) in the central parietal electrode were as follows: for the first peak: gamma 330 ms, SD 49; beta 1: 288 ms, SD 50; and beta 2: 301 ms, SD 65; and for the second peak: gamma: 684 ms, SD 70; beta 1: 684 ms, SD 50; beta 2: 663 ms, SD 45. There were no significant differences between gamma and beta latencies ($t_{(9)} < 1.84, P > 0.099$, $t_{(9)} < 0.83, P > 0.427$, for early and late peaks, respectively).

In addition to the predicted changes in gamma and beta oscillations, there was also a significant stimulus effect in the alpha band ($F_{(1,9)} = 9.0, P = 0.015$) for peak 1 and in trend ($F_{(1,9)} = 4.7, P = 0.059$) for peak 2 (Fig. 2). While the latency of the early alpha peak was not different from that of gamma and beta ($t_{(9)} < 1.24, P > 0.246$), the late alpha activity occurred with a delay of more than 100 ms ($t_{(9)} < 5.46, P < 0.001$).

Correlation Between Gamma and Beta Activity. Finally, we investigated whether the magnitude of gamma activity correlated with the magnitude of beta 1 activity as predicted from *in vitro* studies (9, 10, 23). We expected that such a correlation would apply particularly to the first, novel, stimulus in each stimulus trial. This prediction was confirmed for both stimulus-evoked (GFP)

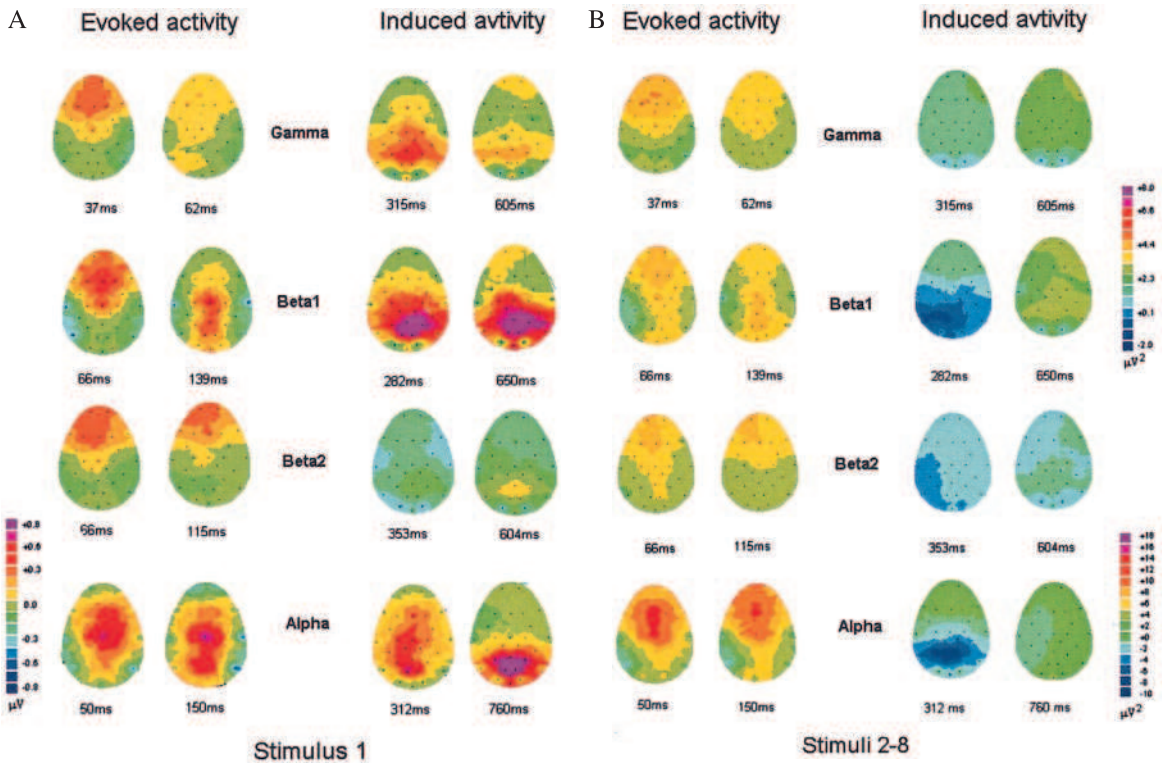

Fig. 3. Topographical maps of the evoked and induced activity for the first stimulus (*A*) and the mean of stimuli 2–8 (*B*) are shown for all four frequency bands. For evoked activity, maps were computed for the two positive peaks around the GFP maximum. For induced activity, maps are shown for the maxima of the early and late induced peaks. Note that the maps of evoked beta 1 exhibit an early fronto-central and a later centro-parietal distribution. Polarity information is not included in the distribution of induced peaks.

activity and for the early peak of the induced oscillatory activity. For evoked GFP this correlation was significant for stimulus 1 (gamma–beta 1: Spearman's $r = 0.73$, $P = 0.016$), but not for subsequent stimuli (gamma–beta 1: $r = 0.04$, $P = 0.907$). There was no significant correlation between gamma and beta 2 activity (for stimulus 1: $r = 0.51$, $P = 0.130$; for stimuli 2–8: $r = 0.09$, $P = 0.803$). The early induced gamma correlated significantly with beta 1 for the first and subsequent stimuli ($r = 0.70$, $P = 0.025$; $r = 0.71$, $P = 0.022$, respectively). For the late peak this correlation was not significant for stimulus 1 ($r = 0.41$, $P = 0.244$); however, it was highly significant for subsequent stimuli 2–8 ($r = 0.95$, $P < 0.001$). This different pattern of correlation suggests that the late induced activity may subserve processes in addition to the initial encoding of novel stimuli.

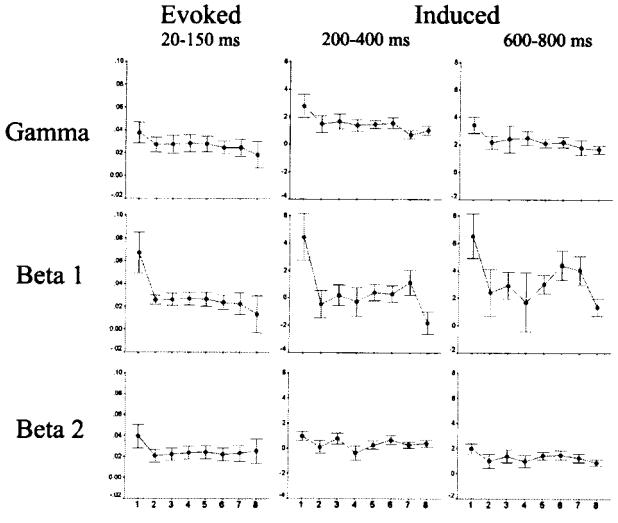

Fig. 4. Mean and standard error are shown for the evoked and induced activity in response to the first eight stimuli in each trial. Response amplitude in the evoked and induced beta 1 band differed significantly between the first, novel, stimulus and the mean of all subsequent stimuli.

Discussion

In vitro studies have characterized a robust pattern of oscillatory responses to afferent stimulation in the hippocampus (9, 10). The response takes the form of an initial period of gamma oscillation followed by a transition, of variable duration, to a beta frequency oscillation. In addition, recent studies have shown that this pattern of oscillatory response habituated markedly when stimuli were presented less than 1 min apart (23). Results from the present study demonstrated that a very similar pattern of transition from gamma to beta oscillations occurs in response to auditory stimulation in the human EEG.

Three observations are critically involved in supporting this statement. First, the initial evoked oscillatory response to novel stimuli took the form of a gamma oscillation, which was either replaced by or superimposed on a longer-lasting beta frequency oscillation (gamma-to-beta shift). For the emergence of oscillatory EEG activity at the scalp a certain level of underlying neuronal synchronization as well as the recruitment of pyramidal cells is necessary. This indicates a superthreshold origin of these oscillations. The transition from gamma to beta oscillation was related to the magnitude of this initial superthreshold gamma oscillation. Second, gamma oscillations were always present (evoked or induced) concurrently with bursts of beta activity.

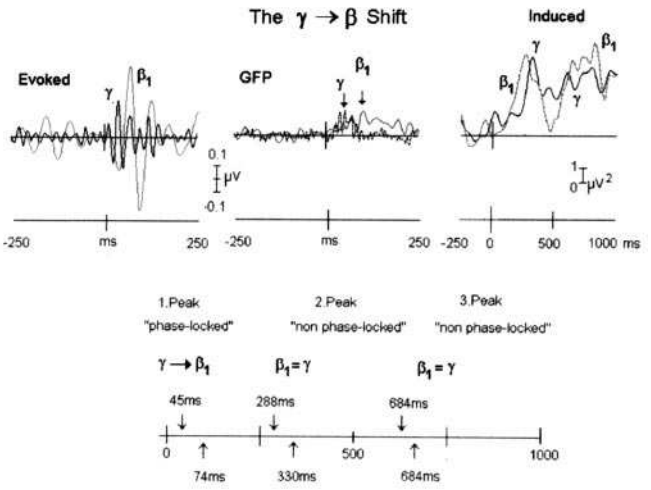

Fig. 5. (*Upper*) The temporal sequence of the early (evoked) and late (induced) oscillatory activity in the gamma and beta 1 band is illustrated. Note that the shift from gamma to beta 1 occurred at the initial phase-locked response, whereas the induced peaks were not significantly different in latency. The time scale and voltage scaling for evoked and induced oscillations differ. (*Lower*) Schematic summary of the temporal sequence using a common time-scale, showing that the gamma-to-beta transition as seen *in vitro* was observed only for the early evoked (phase-locked) peak. There were no significant differences between the late induced gamma and beta 1 bands in peak latency.

The beta activity that correlated with gamma (30–50 Hz) was in the beta 1 range (12–20 Hz) not the beta 2 range (20–30 Hz). This observation suggests that the beta 1 oscillations represent a subharmonic of the on-going gamma and not simply a slowing-down of the gamma frequency response, and accordingly corresponds to what is seen *in vitro* (9, 10). Finally, in the present protocol novel auditory stimuli were followed by repeated identical stimuli. Both gamma and beta oscillations habituated markedly after the initial novel presentation. This effect was particularly apparent for oscillations in the beta 1 band, also consistent with *in vitro* observations (23).

The above comparisons have yielded some intriguing similarities. However, conclusions based on comparison between *in vitro* preparations and the human EEG must remain tentative at present in view of considerable differences between the methods. For example, the activity recorded *in vitro* was predominantly induced in nature (i.e., not strictly phase-locked to the stimulus), compared with a mixture of both stimulus-evoked and -induced activity in the human recordings. Also, the exact nature of the stimulation protocol used in both studies is analogous at best. We used loud auditory stimuli to resemble the high stimulation intensity needed to elicit beta oscillation in the hippocampal slice. For the human experiment, sudden changes in tone frequency were assumed to provide stimulus novelty. In contrast, during the *in vitro* recordings novelty was thought to be served by alternating from proximal to distal stimulation (recording) sites in the rat hippocampal CA1 region (23). Also, the time scale of stimulation was different for the human experiment and the recording in the slice, reflecting optimal conditions for eliciting oscillatory activity in these two different experimental situations. It is also likely that there is at least some difference in the generation of fast oscillations in the hippocampal cortex (archicortex) and neocortex, and that there are species differences between rodents and humans. Furthermore, although the correlation between single-cell and population activity is firmly established (10), the sources of such activity in the human EEG are less well established (13, 20). Nevertheless, the prediction derived from the experimental and the theoretical model provides a firm basis for the understanding of analogous phenomena in the human EEG.

The fronto-central scalp distribution of the early evoked gamma and beta oscillations was consistent with previous studies implicating bilateral dipole sources located in the auditory cortex within the superior temporal gyrus (13). The later induced gamma and beta oscillations were elicited with peaks at 300 ms and 680 ms over central posterior electrodes, suggesting sources within the parietal association areas. Very similar bimodal peaks of induced gamma activity at 300 ms and 500 ms were observed by Tallon-Baudry and Bertrand (20) over parietal regions in an auditory target detection task. Notwithstanding that the induced activity was extracted after rectification of the EEG (thereby losing polarity information), it is still evident that separate regions were involved in the generation of early evoked compared with late induced activity. Our data do not directly address the question of the functional interaction between early activation of the auditory cortex and the later activity over the posterior association cortex implicated in novelty detection and attention (30, 31). It is therefore of interest that the evoked beta 1 activity, occurring initially with a frontal distribution, appeared to shift to a centro-parietal maximum (Fig. 3) during the later phase of this evoked oscillation. Importantly, this shift can be observed only for evoked beta 1 activity, not for gamma and beta 2. Although no firm conclusion about the cerebral generators can be drawn from surface EEG data without combining them with source localization methods, it will be important to establish whether this topographical shift is related to the long-range synchronizing properties of beta oscillations as predicted by Koppell *et al.* (11).

Experimental protocols similar to the protocol used in the present study commonly elicit MMN potentials between 80 and 200 ms over the frontal scalp as the earliest discriminatory ERP (29, 32). MMN reflects an automatic (preattentive) comparison in sensory memory between the incoming stimulus and a memory trace of the preceding stimuli. With large frequency separation between the stimuli as in this experiment, the MMN is superimposed on the N1 component (28, 29), reflecting overlap of two separate components: refractoriness of the N1 generator and a true MMN. MMN and N1 peaked at approximately 105 ms poststimulus (shown as difference waves in Fig. 1), which was 30 ms later than the peaks of beta 1 activity, and 60 ms later than gamma. No significant stimulus effects were observed in the gamma response. The significant stimulus effect observed in beta 1, therefore represents an even earlier discriminatory response than the MMN. Post-hoc comparison showed that the beta 1 GFP latency was significantly shorter than the N1 peak latency ($t_{(9)} = 3.32$, $P = 0.009$). Thus, the present results are in agreement with previous reports that failed to find significant stimulus effects in the gamma band response before 100 ms (33–35). However, the current data showed that stimulus-specific encoding of novel or deviant stimuli resulted in enhanced beta 1 oscillations, which has not been investigated previously. Nevertheless, there is evidence that attention and expectancy can enhance this early gamma response, suggesting a role for top-down modulation (36–38).

The relationship between gamma and beta oscillations points to a number of cognitive correlates. Sokolow (39) and Darrow *et al.* (40) discovered that beta oscillations appeared in the human EEG in response to novel stimuli that also elicited an "orienting response." It remains to be investigated whether the electrodermal orienting response (30, 41) shows a pattern of habituation similar to that of the gamma–beta frequency shifts recorded in this study.

It has been argued that the early evoked gamma band response could reflect the initial coactivation of neuronal assemblies representing specific stimulus features (binding) (20). A change

in such feature configuration by a novel stimulus would be detected at the level of the auditory cortex. The present data suggest that this detection mechanism is reflected in a burst of beta 1 oscillations. A similar role for gamma-induced beta oscillations in novelty detection was postulated on the basis of *in vitro* data (9). In the latter case synchronous beta oscillations were generated as a consequence of potentiation of excitatory synaptic connections between pyramidal cells afforded by the initial synchronous gamma oscillation. In the hippocampal slice model this phenomenon takes approximately 10 periods of gamma oscillation to produce the required potentiation. In the present study this appears to occur over 2–5 periods of gamma. This temporal difference may reflect the greater occurrence of recurrent excitatory synaptic connectivity in the neocortex in comparison with the hippocampus.

The following scenario of processing steps can be postulated. Stimulus novelty detected in the auditory cortex is "flagged" to posterior association areas by means of a synchronous oscillation in the beta 1 range, which then entrains local inhibitory networks at gamma frequency (11). This may explain why induced beta 1 activity over the parietal cortex peaked slightly earlier than gamma. It still needs to be established whether this mechanism is specific to the beta frequency range. In human experiments thalamo–cortical interactions in the alpha range are likely to occur. This may account for the observed stimulus effects on induced alpha activity. However, as in other studies (reviewed in ref. 20), differences in latency and topography suggest that the gamma and beta oscillations are not artifacts of alpha harmonics as previously argued (16).

In conclusion, despite differences in method there was a considerable degree of consistency between the two levels of experimental analysis. This study demonstrates that the pattern of interplay between gamma and beta (specifically beta 1) oscillations is similar in neocortical responses to auditory stimulation to that seen *in vitro* in the hippocampal slice preparation. Both show (*i*) a degree of dependence on gamma oscillations for the generation of beta responses and (*ii*) a very similar pattern of habituation to repeated stimulation, which suggest that they may be involved in processes associated with encoding into sensory memory both at the cellular level (synaptic potentiation) and at the cognitive level (ERP: MMN). These data demonstrate a robust phenomenon allowing the study of the interrelationship between gamma and beta oscillations in humans. The similarities between these findings and observations from *in vitro* studies suggest that a combination of these approaches will facilitate detailed pharmacological and psychophysiological investigations into the mechanisms of the generation and function of fast oscillations in the central nervous system.

We thank Dr. Mark Pflieger for helpful discussion and support with the instantaneous frequency analysis. This study was supported by grants from the Institut für Grenzgebiete der Psychologie und Psychohygiene, Freiburg, Germany, and The Wellcome Trust.

1. Barth, D. S. & MacDonald, K. D. (1996) *Nature (London)* **383,** 78–81.
2. Roelfsema, P. R., Engel, A. K., Konig, P. & Singer, W. (1997) *Nature (London)* **385,** 157–161.
3. Rodriguez, E., George, N., Lachaux, J. P., Martinerie, J., Renault, B. & Varela, F. J. (1999) *Nature (London)* **397,** 430–433.
4. Miltner, W. H., Braun, C., Arnold, M., Witte, H. & Taub, E. (1999) *Nature (London)* **397,** 434–436.
5. Gray, C. M. & McCormick, D. A. (1996) *Science* **274,** 109–113.
6. Whittington, M. A., Traub, R. D. & Jefferys, J. G. (1995) *Nature (London)* **373,** 612–615.
7. MacDonald, K. D., Fifkova, E., Jones, M. S. & Barth, D. S. (1998) *J. Neurophysiol.* **79,** 474–477.
8. Buhl, E. H., Tamas, G. & Fisahn, A. (1998) *J. Physiol. (London)* **513,** 117–126.
9. Whittington, M. A., Traub, R. D., Faulkner, H. J., Stanford, I. M. & Jeffreys, J. G. R. (1997) *Proc. Natl. Acad. Sci. USA* **94,** 12198–12203.
10. Traub, R. D., Whittington, M. A., Buhl, E., Jeffreys, J. G. R. & Faulkner H. J. (1999*) J. Neurosci.* **19,** 1088–1105.
11. Kopell, N., Ermentrout, B. E., Whittington, M. A. & Traub, R. D. (2000*) Proc. Natl. Acad. Sci. USA* **97,** 1867–1872.
12. Von Stein, A., Rappelsberger, P., Sarnthein, J. & Petsche, H. (1999) *Cerebral Cortex* **9,** 137–150.
13. Pantev, C., Makeig, S., Hoke, M., Galambos, R., Hampson, S. & Gallen, C. (1991) *Proc. Natl. Acad. Sci. USA* **88,** 8996–9000.
14. Galambos, R., Makeig, S. & Talmachoff, P. J. (1981) *Proc. Natl. Acad. Sci. USA* **78,** 2643–2647.
15. Tallon-Baudry, C., Bertrand, O., Delpuech, C. & Pernier, J. (1996) *J. Neurosci.* **16,** 4240–4249.
16. Juergens, E., Roesler, F., Henninghausen, E. & Heil, M. (1995) *Neuroreport* **6,** 813–816.
17. Clementz, B. A., Blumenfeld, L. D. & Cobb, S. (1997) *Neuroreport* **8,** 3889–3893.
18. Basar, E., Rosen, B., Basar-Eroglu, C. & Greitschus, F. (1987) *Int. J. Neurosci.* **33,** 103–117.
19. Karakas, S. & Basar, E. (1998) *Int. J. Psychophysiol.* **31,** 13–31.
20. Tallon-Baudry, C. & Bertrand, O. (1999) *Trends Cogn. Sci.* **3,** 151–162.
21. Pfurtscheller, G. (1988) *Electroencephalogr. Clin. Neurophysiol.* **70,** 190–193.
22. Pulvermueller, F., Keil, A. & Elbert, T. (1999) *Trends Cogn. Sci.* **3,** 250–252.
23. Doheny, H. C., Faulkner, H. J., Gruzelier, J. H. & Whittington, M. A. (2000) *J. Physiol.,* in press.
24. Lehmann, D. & Skrandies, W. (1986) *Electroencephalogr. Clin. Neurophysiol.* **48,** 609–621.
25. Thatcher, R. W., Toro, C., Pflieger, M. E. & Hallet, M. (1994) in *Functional Neuroimaging: Technical Foundations*, ed. Thatcher, R. W. (Academic, San Diego), pp. 269–278.
26. Thatcher, R. W. (1995) *J. Neuroimaging* **5,** 35–45.
27. Naatanen, R. (1992) *Attention and Brain Function* (Erlbaum, Hillsdale, NJ).
28. Scherg, M., Vasjar, J. & Picton, T. W. (1989) *J. Cogn. Neurosci.* **1,** 336–355.
29. Baldeweg, T., Richardson, A., Watkins, S., Foale, C. & Gruzelier, J. (1999) *Ann. Neurol.* **45,** 495–503.
30. Knight, R. T. & Nakada, T. (1998) *Rev. Neurosci.* **9,** 57–70.
31. Yamaguchi, S. & Knight, R. T. (1991) *J. Neurosci.* **11,** 2039–2054.
32. Naatanen, R. & Winkler, I. (1999) *Psychol. Bull.* **125,** 826–859.
33. Tiitinen, H., Sinkkonen, J., May, P. & Naatanen, R. (1994) *Neuroreport* **6,** 190–192.
34. Joliot, M., Ribary, U. & Llinas, R. (1994) *Proc. Natl. Acad. Sci. USA* **91,** 11748–11751.
35. Marshall, L., Moelle, M. & Bartsch, P. (1996) *Neuroreport* **7,** 1517–1520.
36. Tiitinen, H., Sinkkonen, J., Reinikainen, K., Alho, K., Lavikainen, J. & Naatanen, R. (1993) *Nature (London*) **364,** 59–60.
37. Makeig, S. & Jung, T. P. (1996) *Brain Res. Cogn. Brain Res.* **4,** 15–25.
38. Herrmann, C. S., Mecklinger, A., Pfeifer, E. (1999) *Clin. Neurophysiol.* **110,** 636–642.
39. Sokolow, N. E. (1963) *Annu. Rev. Physiol.* **25,** 545–580.
40. Darrow, C. W., Vieth, R. N. & Wilson, J. (1957) *Science* **126,** 74–75.
41. Gruzelier, J., Eves, F., Connolly, J. & Hirsch, S. (1981) *Biol. Psychol.* **12,** 187–209.